MASS LOADING COMPENSATION FOR FREQUENCY RESPONSE FUNCTION MEASUREMENTS BY INVERSE RCSA

Kadir Kiran[a,b], Harsha Satyanarayana[b], Chang Kyu Song[b,c], and Tony L. Schmitz[b]
[a]Department of Mechanical Engineering, Suleyman Demirel University, Turkey
[b]Department of Mechanical Engineering and Engineering Science, University of North Carolina at Charlotte, Charlotte, NC, USA
[c]Department of Ultra Precision Machines and Systems, Korea Institute of Machinery and Materials, Korea

INTRODUCTION

Machining operations can be stable or unstable depending on the cutting parameters and machine-spindle-holder-tool assembly frequency response function (FRF). In some cases, the workpiece FRF can influence the machining behavior as well. Stable, or chatter-free, cutting conditions can be predicted using process stability models [1]. These models require the machine-spindle-holder-tool assembly FRF (and sometimes the workpiece FRF). System FRFs can be obtained by measurement (i.e., modal testing) or models (analytical and/or numerical methods). Schmitz and Donaldson [2] first presented the Receptance Coupling Substructure Analysis (RCSA) method to predict machine-spindle-holder-tool assembly FRFs by coupling individual component FRFs (or receptances). This method reduces measurement time because assembly FRFs can be predicted rather than measured. Subsequent publications have improved the technique [3-12].

In this paper a novel application of RCSA is presented in order to improve FRF measurement accuracy. In modal testing, FRFs are measured using an instrumented hammer to excite the system and (typically) an accelerometer to record the response. However, the measured FRF differs slightly from the actual FRF due to the accelerometer and cable mass. In order to compensate for this mass loading, the inverse RCSA approach is applied here.

RCSA BACKGROUND

RCSA is used to predict an assembly's receptances by coupling receptances from the individual components. The connections between components can be rigid or flexible with or without energy dissipation (damping) [13]. An example for rigid coupling of two components is displayed in Fig. 1.

For this example, the component direct receptances can be described as $h_{1a1a} = x_{1a}/f_{1a}$ (component I) and $h_{1b1b} = x_{1b}/f_{1b}$ (component II). The compatibility condition for the rigid coupling is $x_{1b} - x_{1a} = 0$. The equilibrium condition, $f_{1a} + f_{1b} = F_1$, relates the internal (component) forces to the external (assembly) forces. The assembly (III) direct receptance, H_{11}, at assembly coordinate, X_1, can be expressed as shown in Eq. 1.

$$H_{11} = \frac{X_1}{F_1} = h_{1a1a} - h_{1a1a}\left(h_{1a1a} + h_{1b1b}\right)^{-1} h_{1a1a} \qquad (1)$$

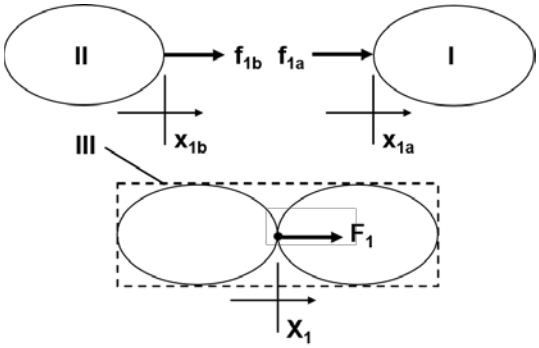

Figure 1. Two component RCSA model: I and II are individual components and III is the assembly.

INVERSE RCSA APPROACH FOR MASS LOADING COMPENSATION

A tool point FRF is measured by modal testing as shown in Fig. 2a. The experimental FRF differs from the actual FRF due to the accelerometer and cable mass. A reduction in the natural frequency(s) and FRF magnitude may be observed, depending on the amount of mass loading.

The accelerometer and cable mass can be compensated using inverse RCSA, where the corresponding RCSA model is depicted in Fig. 2b. In this model, it is assumed that accelerometer is rigidly coupled to the tool point. The measurement provides the assembly receptance, $H_{11} = X_1/F_1$. The accelerometer/cable receptance is $h_{1a1a} = x_{1a}/f_{1a}$, while the unknown tool point receptance is $h_{1b1b} = x_{1b}/f_{1b}$. The tool point receptance can be determined by rearranging Eq.1 as shown in Eq. 2. This approach is

referred to as inverse RCSA since it is a decoupling, rather than a coupling, step.

$$h_{1b1b} = -h_{1a1a} + h_{1a1a}\left(h_{1a1a} - H_{11}\right)^{-1} h_{1a1a} \qquad (2)$$

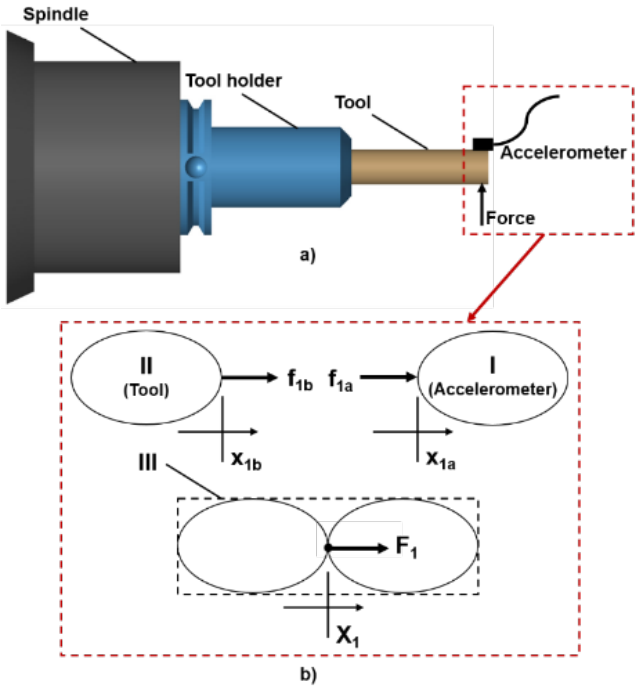

Figure 2. a) FRF measurement and b) RCSA model.

For this study, the accelerometer/cable is defined as a point mass. The corresponding receptance is provided in Eq. 3, where m is the mass and ω is the frequency (rad/s).

$$h_{1a1a} = -1/\left(m\omega^2\right) \qquad (3)$$

Figure 3. 12.7 mm diameter rod setup.

RESULTS

Experiments were performed on two setups: 12.7 mm diameter and 6.35 mm diameter steel rods clamped at one end in a cantilever configuration. Figure 3 displays a photograph of the 12.7 mm diameter rod measurement platform. A split clamp was used to hold the tool at the desired cantilever length. The 6.35 mm diameter rod was clamped in an ER16 collet holder with a CAT-40 interface, which was then secured using a manual draw bolt in a spindle nose attached to a large steel block; see Fig. 4.

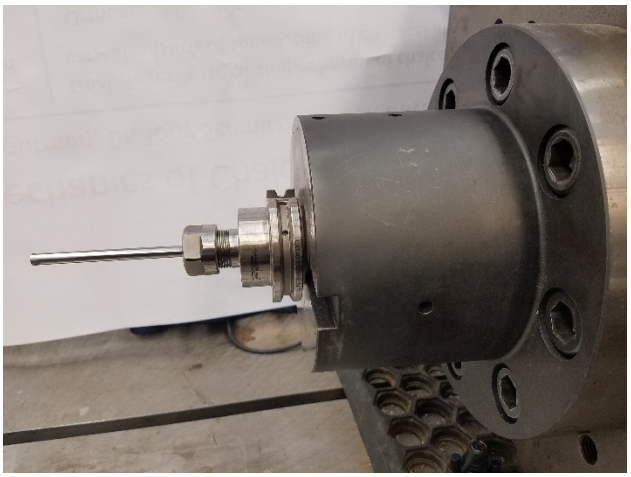

Figure 4. 6.35 mm diameter rod setup.

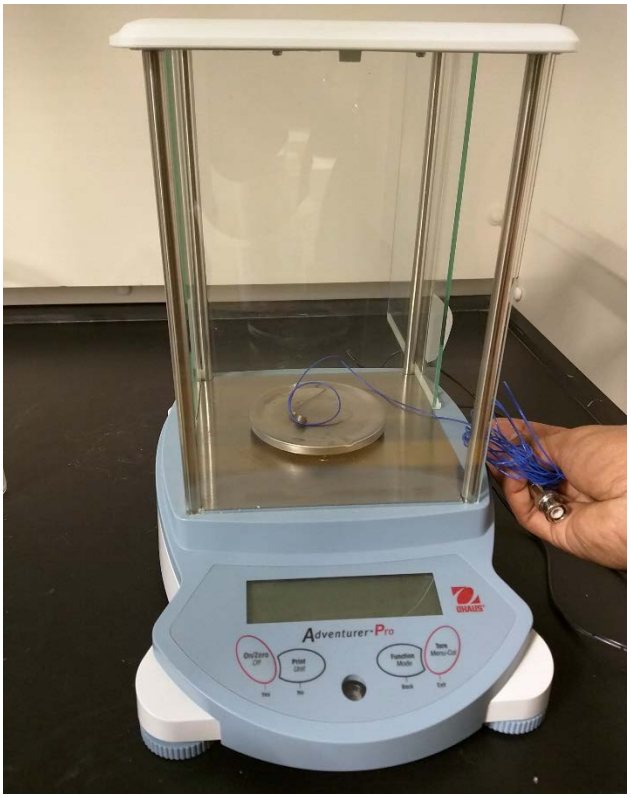

Figure 5. Accelerometer-cable mass measurement.

For both rod diameters, multiple stickout lengths were selected and measurements were performed with: a medium-size accelerometer (PCB 352A21), a small-size accelerometer (PCB 352C23), and a laser vibrometer (Polytec OFV-534). To obtain the accelerometer/cable masses, measurements were performed using an Ohaus AV264C Adventurer ProAnalytical Balance (0.1 mg resolution). A measurement example is displayed in Fig. 5, where the accelerometer, approximate catenary length of the cable from the tool point measurement (for the cable mass), and the modal wax were included.

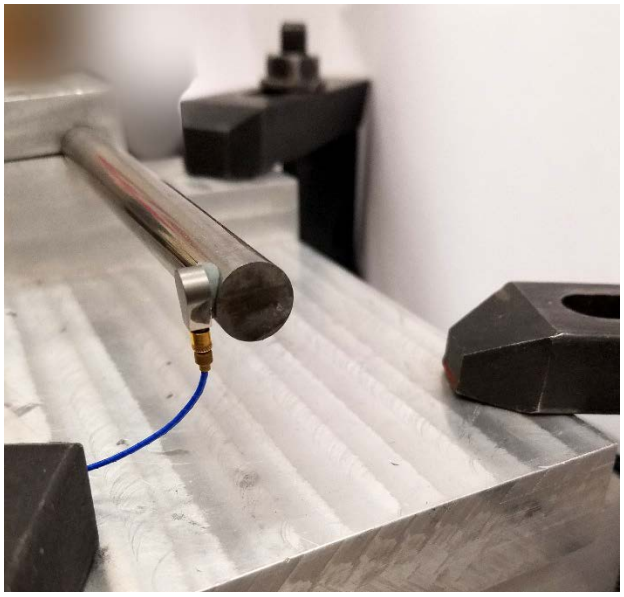

Figure 6. Medium accelerometer attached to the 12.7 mm diameter rod using modal wax.

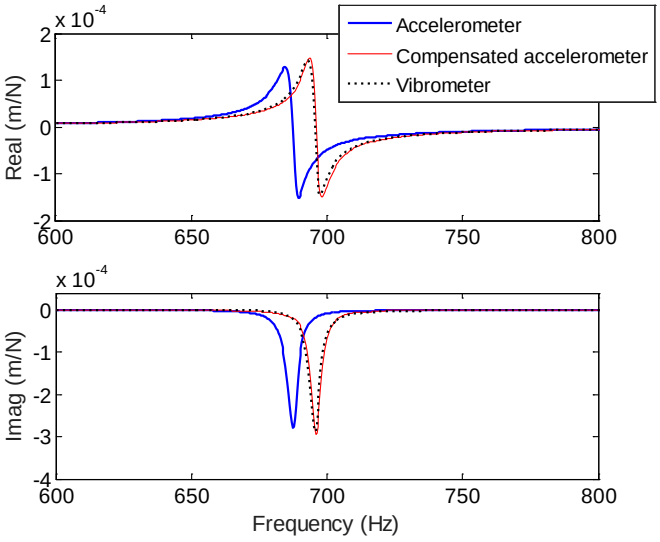

Figure 7. Results for 12.7 mm diameter rod with a stickout length of 102 mm using the medium accelerometer.

Figure 6 shows the medium accelerometer attachment for a stickout length of 102 mm for the 12.7 mm diameter rod. The measurement and compensation results are displayed in Fig. 7, where the accelerometer/cable mass was 706 mg. It is seen that the accelerometer FRF has a lower natural frequency than the vibrometer (non-contact) FRF. Using Eq. 2 and the measured mass, the mass loaded FRF is compensated to remove the mass loading effect. This result matches closely with the vibrometer result (phase error in the vibrometer measurement due to a time delay between the hammer and vibrometer electronics was compensated using the technique described in [14]).

A summary of 12.7 mm diameter rod measurement results for both accelerometers at four different stickout lengths is provided in Table 1.

Table 1. 12.7 mm diameter rod results.

Stick-out (mm)	Vibro. freq. (Hz)	Accel. freq. (Hz)	% error	Comp. freq. (Hz)	% error
Medium accelerometer (706 mg)					
102	695.4	687.4	1.10	695.8	-0.05
111	597.8	592	0.97	598.5	-0.11
118	538.3	533.3	0.92	537.5	0.15
124	492.1	487.1	1.01	492.1	0
Small accelerometer (275 mg)					
102	698.1	695	0.44	698.1	0
111	613.8	611.5	0.37	614.2	-0.06
118	555.4	552.8	0.46	555	0.07
124	503	501.3	0.33	502.8	0.03

*Stickout lengths are approximate. Different setups were used between the small and medium accelerometers.

Figure 8. Small accelerometer attached to the 6.35 mm diameter rod using modal wax.

Figure 8 shows the small accelerometer attached to the 6.35 mm diameter rod. Measurement results are presented in Table 2.

Table 2. 6.35 mm diameter rod results.

Stick-out (mm)	Vibro. freq. (Hz)	Accel. freq. (Hz)	% error	Comp. freq. (Hz)	% error
Medium accelerometer (680 mg)					
79	687.8	671.0	2.4	688.2	-0.06
89	545.5	532.2	2.4	545.9	-0.07
Small accelerometer (275 mg)					
79	688.2	646.0	6.1	688.9	-0.10
89	546.3	516.0	5.5	547	-0.12

*Stickout lengths are approximate. Different setups were used between the small and medium accelerometers.

CONCLUSIONS

This paper described the application of inverse Receptance Coupling Substructure Analysis (RCSA) to mass compensation for accelerometer-based impact testing. The measurement (assembly) FRF was used together with a point mass model for the accelerometer/cable to determine the compensated tool point FRF. Experiments were completed for two tool diameters and multiple stickout lengths for a cantilever configuration. The average percent error in fundamental natural frequency after compensation was -0.03%.

ACKNOWLEDGEMENTS

The authors gratefully acknowledge the Scientific and Technological Research Council of Turkey (TUBITAK) 2214/A International Doctoral Research Fellowship Programme for a research scholarship to the author, Kadir Kiran, in order to perform research at UNC Charlotte.

REFERENCES

[1] Schmitz, T. L. and Smith, K. S., 2009. Machining Dynamics: Frequency Response to Improved Productivity. Springer, New York, NY.

[2] Schmitz T.L. and Donaldson R.R., 2000. Predicting High-Speed Machining Dynamics by Substructure Analysis. CIRP Annals-Manufacturing Technology, 49 (1), 303-308.

[3] Schmitz, T., Davies, M., Medicus, K., and Snyder, J., 2001. Improving High-Speed Machining Material Removal Rates by Rapid Dynamic Analysis. Annals of the CIRP, 50/1: 263-268.

[4] Schmitz, T., Davies, M., and Kennedy, M., 2001. Tool Point Frequency Response Prediction for High-Speed Machining by RCSA. Journal of Manufacturing Science and Engineering, 123: 700-707.

[5] Duncan, G.S., Tummond, M., and Schmitz, T., 2005. An Investigation of the Dynamic Absorber Effect in High-Speed Machining. International Journal of Machine Tools and Manufacture, 45: 497-507.

[6] Schmitz, T. and Duncan, G.S., 2005. Three-Component Receptance Coupling Substructure Analysis for Tool Point Dynamics Prediction. Journal of Manufacturing Science and Engineering, 127/4: 781-790.

[7] Schmitz, T. and Duncan, G.S., 2006. Receptance Coupling for Dynamics Prediction of Assemblies with Coincident Neutral Axes. Journal of Sound and Vibration, 289/4-5: 1045-1065.

[8] Schmitz, T., Powell, K., Won, D., Duncan, G.S., Sawyer, W.G., and Ziegert, J., 2007. Shrink Fit Tool Holder Connection Stiffness/Damping Modeling for Frequency Response Prediction in Milling, International Journal of Machine Tools and Manufacture. 47/9: 1368-1380.

[9] Cheng, C.-H., Duncan, G.S., and Schmitz, T., 2007. Rotating Tool Point Frequency Response Prediction using RCSA. Machining Science and Technology, 11/3: 433-446.

[10] Filiz, S., Cheng, C.-H, Powell, K., Schmitz, T., and Ozdoganlar, O., 2009. An Improved Tool-Holder Model for RCSA Tool-Point Frequency Response Prediction. Precision Engineering, 33: 26-36.

[11] Schmitz, T., 2010. Torsional and Axial Frequency Response Prediction by RCSA. Precision Engineering, 34: 345-356.

[12] Kumar, U. and Schmitz, T., 2012. Spindle Dynamics Identification for Receptance Coupling Substructure Analysis. Precision Engineering, 36/3: 435-443.

[13] Schmitz, T.L. and Smith, K.S., 2012. Mechanical Vibrations: Modeling and Measurement. Springer, New York, NY.

[14] Ganguly V. and Schmitz T.L., 2014. Phase Correction for Frequency Response Function Measurements. Precision Engineering, 38, 409-413.